OBSERVED 1970-2005 COOLING OF SUMMER DAYTIME TEMPERATURES IN COASTAL CALIFORNIA

Bereket Lebassi, Jorge Gonzalez, and Drazen Fabris
Department of Mechanical Engineering, Santa Clara University, Santa Clara, California

Edwin Maurer
Department of Civil Engineering, Santa Clara University, Santa Clara, California

Norman Miller
Climate Science Department, Lawrence Berkeley National Laboratory, Berkeley, California

Cristina Milesi
Foundation, California State University, Monterey Bay, Monterey, California
at NASA Ames Research Center, Mountain View, California

Robert Bornstein
Department of Meteorology, San José State University, San José, California

---

Corresponding author address: Jorge Gonazalez, Santa Clara University, 500 El Camino Real, Santa Clara, CA 95053.
E-mail: jgonzalezcruz@scu.edu

ABSTRACT

The study evaluated 1948-2004 summer (JJA) mean monthly air temperatures for two California air basins: SoCAB and SFBA. The study focuses on the more rapid post-1970 warming period, and its daily T_{min} and T_{max} values were used to produce average monthly values and spatial distributions of trends for each air basins. Additional analyses included T_D values at two NWS sites, SSTs, NCEP reanalysis sea-level pressures, and GCM T_{ave}-values.

Results for all California COOP sites together showed increased JJA T_{ave}-values; asymmetric warming, as T_{min}-values increase faster than T_{max}-values; and thus decreased DTR values. The spatial distribution of observed SoCAB and SFBA T_{max} values exhibited a complex pattern, with cooling in low-elevation coastal-areas open to marine air penetration and warming at inland areas. Results also showed that decreased DTR values in the valleys arose from small increases at "inland" sites combined with large decreases at "coastal" sites.

Previous studies suggest that cooling JJA T_{max}-values in coastal California were due to increased irrigation, coastal upwelling, or cloud cover, while the current hypothesis is that they arises from GHG-induced global-warming of "inland" areas, which results in increased sea breeze flow activity. Sea level pressure trends showed increases in the oceanic Pacific High and decreases in the central-California Thermal Low. The corresponding gradient thus showed a trend of 0.02 hPa 100-km^{-1} decade^{-1}, supportive of the hypothesis of increased sea breeze activeity. Trends in T_D values showed a larger value at coastal SFO than at inland SEC, which indicative of increased sea breeze activity; calculated SST trends (0.15^{o}C decade^{-1}) could also have increase T_D-values. GCM model T_{ave}-values showed warming that decreases from 0.13^{o}C decade^{-1} at inland California to 0.08^{o}C decade^{-1} at coastal areas.

Significant societal impacts may result from this observed "reverse-reaction" to GHG-warming, i.e., the decreased JJA T_{max}-values in coastal areas. Possible beneficial effects include decreased: maximum O_3 levels, human thermal-stress, and energy requirements for cooling.

1. Introduction

Daily long term 2-m air temperature trends generally show diurnal asymmetric warming rates, as nighttime minima temperatures T_{min} have warmed faster than daytime maxima T_{max}, which thus decreases daily temperature ranges (DTRs). Karl et al. (1993) attributed this effect to increased evaporation from increased sea surface temperatures (SSTs), which resulted in increased relative humidity and cloud cover; and thus in decreased incoming solar radiation and T_{max}. The radiative-convective model of Stenchikov and Robock (1995) showed that solar reflection and absorption by aerosols also reduced T_{max} warming rates. The Walters et al. (2007) model of stable nocturnal boundary layers (SNBLs) showed that increased greenhouse gases (GHGs) reduce nocturnal IR cooling and thus increase T_{min} values.

Asymmetric warming has also been attributed to anthropogenic land cover conversions on global (Mintz 1984; Zhang 1997) and regional (Chase et al. 2000) scales, e.g., deforestation increases T_{min} (Lawton et al. 2001; Defries et al. 2002; Nair et al. 2003), as do urban heat islands (UHIs, Bornstein 1968; Landsberg 1981; Gallo et al. 1993; Pon et al. 2000). Irrigation decreases T_{max} (Betts 2001), as it converts arid regions to (slower-warming) moist high thermal-inertia vegetated plains (Pielke et al. 2000, 2007). Output from four regional climate models was used by Kueppers et al. (2007) to show that western-US irrigation lowers T_{ave} and T_{max} values at rates comparable to increases from GHG warming. Modeling by Lobell et al. (2006) showed temperature changes generally dominated by GHG warming, but that large fractional land-use changes can dominate in sub-domains.

Regional climate modeling by Snyder et al. (2003) showed that increased GHGs also enhance coastal upwelling by increasing land-ocean pressure and temperature gradients, as land areas warm faster than ocean areas due to thermal differences. The increased gradients also

enhance alongshore winds that produce upwelling, which further increases onshore temperature gradients. McGregor et al. (2007) observed this effect over coastal northwest Africa, while Bakun (1990) had hypothized a similar scenario to explain an observed 30 year increase of upwelling along California. Alfaro et al. (2004) found average March to May Pacific Decadal Oscillation (PDO) values and June to August (JJA) SSTs correlated with JJA T_{ave}-values, with maximum correlations in coast regions. LaDochy et al. (2007) found similar results, but also showed that T_{max} and PDO values were uncorrelated.

Analysis of 80 years of annual-averaged T_{ave} daily values at 112 National Weather Service (NWS) Cooperative (COOP) sites in California by Goodridge (1991) showed warming in coastal (attributed to warming SSTs) and inland urban (attributed to UHI effects) areas; his observed cooling in inland rural areas was unexplained. Nemani et al. (2001) found summertime asymmetric warming at northern California COOP sites in the Napa and Sonoma Valleys during 1951-97, as T_{min} values increased (at $0.44^{o}C$ $decade^{-1}$) and T_{max} values slightly decreased; both effects were attributed to a measured increase in cloud cover. Increased annual dew point temperatures (T_D) over coastal California (at $0.21^{o}C$ $decade^{-1}$) were related to increased SST values.

Interpolated (to a grid) California COOP monthly-averaged T_{ave} values from 1950-99 by Duffy et al. (2006) showed warming in all seasons (average rate of about $0.4^{o}C$ $decade^{-1}$), attributed to increased UHIs or GHGs. Christy et al. (2006) analyzed 1910-2003 data from 18 Central Valley (CenV) COOP sites and showed increased T_{ave} and T_{min} values in all seasons, with greater summer and fall increases. They also found concurrent summer cooling T_{max} (at $-0.26^{o}C$ $decade^{-1}$) and warming dew point T_D (at $0.4^{o}C$ $decade^{-1}$) values, with changes attributed to increased summer irrigation. Bonfils and Duffy (2007) argued, however, that the warming T_{min} values were not due to irrigation, which they said could only overcome GHG-warming

effects on T_{max}. Bonfils and Lobell (2007) showed that expanded irrigation cooled these summer T_{max} values by –0.14 to –0.25°C decade^{-1}, while producing negligible effects on T_{min} values.

The analysis by LaDochy et al. (2007) of data from 331 California COOP sites during 1950-2000 also showed annual T_{ave} values warming at most stations. Almost all increases were due to changes in T_{min}, as T_{max} showed either no change or cooling; fastest T_{min} increases occurred in summer. While maximum T_{ave} warming occurred in southern California areas, its northeast Interior Basin showed cooling (at -0.12^{o}C decade^{-1}). Abatzoglou (2008) also found significant negative trends in late summer-early fall T_{max} values along the immediate California coast over the last three decades.

While previous studies have generally attributed observed decreased summer maximum temperatures during the last decades at COOP sites in coastal California to increases in UHIs, cloud cover, upwelling, and/or irrigation, the current study uses the same data to determine the spatial distributions of these decreases in two important California air basins and to relate them to sea breeze induced marine-air penetration patterns. In addition, the study provides evidence that on-shore breezes have increased during the study period. The paper focuses on two highly populated near sea-level coastal California regions: South Coast Air Basin (SoCAB) and Central California [i.e., San Francisco Bay Area (SFBA) and northern CenV].

2. Methodology

The study evaluates 1970-2004 JJA mean monthly 2-m air temperatures for the above two air basins (Fig. 1). Data were obtained from the National Climate Data Center (NCDC) for 273 COOP sites, including: 58 CenV, 100 Central California, and 30 SoCAB sites. Only daily T_{min} and T_{max} values are used, as hourly values are not available from COOP sites. Even though the data extends back to 1948 at most sites, the shorter sub-period is used as the study focuses on the

more rapid post-1970 warming period, as discussed below. Daily-average temperatures were used to produce average monthly T_{min}, T_{max}, and T_{ave} values. Months with more than five days of missing data and/or sites with less than 15 years of data were excluded. Trends of these variables were calculated for each site, all sites combined, and the coastal and inland sub-regions.

An objective means to detect climate inhomogeneities in monthly-mean T_{min}, T_{max}, and T_{ave}-values at COOP stations across California was developed by Abatzoglou et al. (2008). They found that, while individual-station inhomogeneities can influence its trends, no widespread or geographically coherent inhomogeneties were identified across the state for 1970 to the present.

The current effort is an exploratory statistical investigation of recent historical observed 2-m air temperature trends in two California regions. It contrasts T_{min} vs. T_{max}, winter vs. summer, and within-region spatial variations of these trends. With such an exploratory study of observed trends, calculations of formal statistical-significance measures are not appropriate (Switzer 2008). Such measures are intended to test whether calculated trends could arise by chance from climatology, but with no change over the period of the observations. In addition, area-average statistics would require construction of spatial correlation functions, a non trivial exercise in complex terrain situations.

The current goal is thus not to claim that the climate has changed based on rejection of a null hypothesis, nor is it to estimate future temperature trends, both of which would require probabilistic statistical modeling of the observed record with associated tests of significance. The goal of this exploratory study is rather to elucidate a richer detail of the observed temperature record than has been done before, for the potential evaluation of California climate change models.

Surface wind data are generally only available at airports, and are not measured by the denser network of COOP sites; hence they do not provide sufficient spatial detail. Concurrent trends

of T_D values were, however, calculated at the NWS sites at San Francisco International (SFO) and Sacramento Executive (SEC) airports (Fig. 2a). As SFO is well within the sea breeze intrusion zone and since SEC is near its average eastern inland boundary (as shown below), their post sea-breeze T_D-trend values at 1700 LT (where LT = UTC minus 7 h during summer daylight savings time periods) were analyzed to evaluate possible changes in marine-intrusion characteristics.

Strong topographic distortions of near-surface flow patterns in the two study air-basins have been documented by observations (Hayes et al. 1984; CARB 1989; MacKay 1997). Spatial distributions of observed temperature trend-values for each air basins were subjectively constructed, with summertime climatological wind patterns from the above references overlaid in the figures to aid their interpretation. Subjective analysis was necessary, as interpolation software cannot fully account for topographic distortions of most meteorological fields (though some can approximate topographic influences on wind flow patterns). Spatial temperature-trend plots are useful for qualitative pattern interpretation, and no station trend-value was "violated" in their construction.

Mean-monthly JJA SSTs along California at a 2.5-degree grid resolution were obtained from NCDC. These Extended Reconstructed SST (ERSST) values, from the International Comprehensive Ocean-Atmosphere Data Set (ICOADS), had been produced by statistical methods that allow for stable reconstructions from sparse data (Smith and Reynolds 2003). The 1950-2005 average SST trend was thus calculated for all ocean areas in Fig. 1.

The 1970 to 2006 spatial-distribution of Central California coastal-to-inland sea-level pressure-gradient trends were calculated by use of average JJA NCEP reanalysis values, avail-able at www. cdc.noaa.gov/datasets/ **NCEP.reanalysis/surface/**. These values are available at 6 h intervals, starting at 0500 LT, and thus 1700 LT values were used, as calculated differences are meant

as an estimate of sea breeze activity. Gradients were calculated from differences between averages in a 5 deg by 5 deg ocean area off central California and a similar land area to its east.

General Circulation Model (GCM) outputs of 2-m summer T_{ave}-values from 11 models for 1950-99 on a 2 by 2 deg grid over California were obtained from the IPCC Fourth Assessment World Climate Research Programme (WCRP) Coupled Model Inter-comparison Project Phase 3 (CMIP3) archive. Average values for the entire period were linearly interpolated to a 0.5 by 0.5 degree grid. Additional details of the analysis are in Maurer (2007).

3. Results

a. Local flow patterns

California summer climate is dominated by atmospheric and oceanic features, which include the General Circulation (GC) Pacific High, coastal ocean current system, and continental thermal low (with an axis from the Mexican plateau to central California). The High creates along-shore wind stresses on the ocean surface, which results in spring and summer upwelling of cold water to the surface (Hickey 1979; Bakun 1990; Herbert and Schuffert 2001; McGregor et al. 2007). Climate variability can produce small changes in these features and thus large variations in coastal climate (Gilliland 1980), e.g., during El Niño years, upwelling diminishes and SSTs increase along California (Simpson 1983).

These features also produce strong pressure, temperature, and moisture gradients, as well as a nearly continuous summer daytime onshore, cool, moist Pacific Coast Monsoon marine airflow (Williams and DeMandel 1966; Giorgis 1983; Miller and Schlegel 2006). Subsidence from the High also produces an elevated inversion layer that caps the shallow (< 1 km deep) marine boundary layer (MBL). The inversion (up to 20^{o}C through a 250 m layer) and its base lowest just off the coast, where upwelling water results in MBL cooling (Seaman et al. 1995).

Knowledge of local topographic effects on marine air intrusions is essential to understanding study-area flow patterns. The CenV of California is about 800 km long and 80 km wide (Fig. 1), with the Sacramento Valley (SacV) as its northern third and the San Joaquin Valley (SJV) its southern two-thirds. It is bordered by a continuous barrier of at least 1500 m in elevation: Klamath Mountains on its northwest, Cascades on its northeast, and Sierra Nevada on its east. Its western border is the Coastal Range (elevation of 915 m), with the following low-elevation inlets from the Ocean into the SacV (Fig. 2a): (a) Golden Gate Gap (GGG), a sea level passage into San Francisco Bay; (b) Estero Lowlands, near sea level and north of San Francisco; and (c) San Bruno Gap, south of San Francisco (elevation of 61 m).

Channeling through the GGG produces a westerly jet, which fans into three branches: southward into the Santa Clara Valley, northward into the Petaluma, Sonoma, and Napa Valleys of Marin, and eastward to the Carquinez Strait (Root 1960). The air in the Strait passes the Sacramento River Delta and goes half-way into the CenV (at its central latitude), where it splits northward into the SacV and southward into the SJV (Blumenthal et al. 1985). This onshore-directed marine flow is augmented by thermally-driven daytime upslope-flows along the east-facing slopes of the coastal and inland mountain ranges (Seaman et al. 1995). As nighttime land surfaces cool more rapidly than the sea, a thus reversed temperature-gradient produces evening offshore-directed land-breeze flows, also augmented by similarly-directed downslope mountain flows along the west-facing slopes.

Analogous SoCAB flow-patterns are dominated by the same GC features. The Basin, however, is a coastal plain open to the ocean, with mountain ranges (peaks to 3000 m) on three sides (Fig. 2b). Resulting daytime onshore-directed marine-air intrusions into the SoCAB are thus more widespread than those into the CenV, and the inland movement of its MBL (with an over-

water depth of about 150 m) resembles a cold front (McElroy and Smith 1991). The onshore marine-flow splits northward into the San Fernando Valley and eastward to Chino, where it splits into northward (towards the San Gabriel and San Bernardino Mountains) and southeastward (towards the Lakeview and Estelle Mountains) directed flows. Marine air can be prevented from exiting the Basin (between the San Gabriel and San Bernardino Mountains) by opposing upper level easterly-flows associated with mesoscale high pressure areas north of that gap (Boucouvula et al. 2003).

b. Warming and cooling trends

This section presents warming and cooling trends found in the current study. A comparison with previous literature results is presented in Section 4, as is a proposed explanation of the current and literature results.

Mean JJA California 1970-2005 over-land 2-m T_{ave}-values show the expected warming (Figs. 3a), with an increase of 0.15^{o}C decade^{-1}. Corresponding T_{min} and T_{max} values also show expected asymmetric warming rates (Figs. 3b,c), with increases of 0.27 and 0.04^{o}C decade^{-1}, respectively. Concurrent DTR values (Fig. 3d) have thus decreased, at a rate of -0.23^{o}C decade^{-1}. Note that the corresponding trends during the preceding 20 years were: 0.10, 0.16, 0.05, and -0.12^{o}C decade^{-1}, respectively. As all of these (except T_{max}, which is seen below as a small difference between two large values) were at least 50% less than corresponding 1970-2005 values, the remainder of the paper thus focuses on trends during the later period.

The spatial distribution of observed SoCAB 1970-2004 JJA T_{max} values (Fig. 4) exhibits a complex pattern, with cooling in low-elevation coastal-areas open to marine air penetration and warming at both inland and higher-elevation coastal areas. Marine air enters at the low-elevation coastal area south of Palos Verdes (Fig. 2b), and then splits northward towards the San Fernando Valley (with a max cooling of -0.99^{o}C decade^{-1}) and eastward towards the Chino hills, where it

splits again. One part flows northward, towards the foothills between the San Gabriel and San Bernardino Mountains, while its southern branch flows past the Lakeview and Estelle Mountains. While these regions thus show cooling, higher elevation inland regions (that lack marine air penetration) show warming, i.e., north of Lakeview (local max of 0.12^{o}C decade^{-1}), San Gabriel and San Bernardino Mountains to the north (local max of 0.41^{o}C decade^{-1}), and Santa Ana Mountains to the southwest (max of 0.64^{o}C decade^{-1}).

Given a data scarcity in some areas, some trend-line segments were placed based on an understanding of topographic influences on near-surface flow patterns, e.g., southern end of the -0.2 K decade^{-1} trend-line in the Estelle Valley was justified by the increasing elevation in that area. The 0.0 K decade^{-1} trend-line section between the San Gabriel and San Bernardino Mountains was likewise placed, while the 0.4 K decade^{-1} dashed trend-line near the San Gabriel Mountain was added for continuity with that over the San Bernardino Mountain. Sites north of the San Fernando Valley would allow for a more precise northern edge of that cooling area.

The averaged daytime JJA warming/cooling rates in SoCAB warming/cooling sub-areas of Fig. 4 unexpectedly show a larger average value for all sites in its coastal-cooling area than for all those in its inland-warming area. The values are -0.33 vs. 0.21 K decade^{-1}, respectively.

As SFBA topography is more complex, so are its concurrent 1970-2004 JJA T_{max} spatial warming and cooling patterns (Fig. 5). As its coastal range almost completely blocks marine air penetration, flow through the GGG (Fig. 2a) into the SFBA splits northward towards the Petaluma, Sonoma, and Napa Valleys and meets southward flowing marine air from the Estero Lowlands; these valleys are thus cooling (local max of -0.69^{o}C decade^{-1}). Some GGG air also flows southward along San Francisco Bay into the Santa Clara Valley; cooling sites thus exist on both sides of the Bay (local max of -0.53^{o}C decade^{-1}). Some of the flow through the GGG also splits off southward into the Livermore Valley, in which all sites are cooling (local max of -0.60^{o}C decade^{-1}). The remainder of this air enters the SacV through the Carquinez Strait, where it splits

at the Montezuma Hills into northward and southward flows (local max cooling of -0.33^{o}C decade^{-1}). The most rapidly cooling area, however, is over Monterey Bay (max of -0.73^{o}C decade^{-1}). As the onshore flow from the Bay and the southward flow from the Santa Clara Valley frequently are prevented from converging by the southern extension of the Santa Cruz Mountains, two separate -0.2^{o}C decade^{-1} isotherms are shown.

Warming regions, however, exist along the eastern side of the SacV and in higher elevation areas on its perimeter. The eastern-edge warming (local max of 0.29^{o}C decade^{-1}) is probably associated with wake effects from the high elevation outcrop south of the Montezuma Hills. Warming is also seen in the hills east of San Francisco Bay (local max of 0.72^{o}C decade^{-1}) and in the coastal hills (local max of 0.50^{o}C decade^{-1}) between the San Francisco and Monterey Bay cooling areas.

Given SFBA topographic complexity and data scarcity, part of one trend-line was again placed based on the physical reasoning discussed above, e.g., the end of -0.2 K decade^{-1} isotherm south of the San Francisco Bay could have been linked with that northeast of its current southern edge. Additional observational sites would be useful to better define the edges of several cooling/warming areas, e.g., some within the mountain area south of the Livermore Valley would allow for more precise location of the northern edge of the 0.2 K decade^{-1} trend-line in the southeastern domain, while additional sites in the SacV Delta would have allowed for more precise location for its 0.0 K decade^{-1} trend-line. Observational sites west of the Petaluma Valley and in the hills west of the Delta would have likewise been useful to show the western edges of their cooling areas.

The averaged daytime JJA warming/cooling rates in SFBA warming/cooling sub-areas of Fig. 5 show a larger value for all inland-warming sites than for all those in its coastal-cooling areas (0.47 vs. -0.16 K decade^{-1}, respectively). This reversal from the SoCAB results (discussed

above) arises due to the increased blockage of marine intrusions in the SFBA by its more complex coastal topography.

As a comparison to the all-California trends in Fig. 3, similar trends were evaluated separately for the combined SFBA and SoCAB T_{max}- warming (i.e., generally inland and a few higher elevation coastal areas) areas (Fig. 6b) and then likewise for their combined T_{max}-cooling (i.e., generally low-elevation coastal) areas (Fig. 6a), hereafter referred to as the "inland" and "coastal" areas, respectively. The T_{min} warming trend was greater in the "coastal" areas than the "inland" areas (0.28 vs. 0.16^{o}C decade^{-1}). Corresponding T_{max}-trends were -0.30^{o}C decade^{-1} for the cooling "coastal" areas and 0.32^{o}C decade^{-1} for the warming "inland" areas.

As combined "inland" warming-area (Fig. 6a) T_{min} and T_{max} values both increased, its T_{ave} values increased at a midway rate (0.24^{o}C decade^{-1}), and as its T_{max}-warming was larger than its T_{min}-warming, its DTR-values increased by 0.16^{o}C decade^{-1}. As corresponding "coastal" T_{min} magnitudes (Fig. 6b) increased with a magnitude similar to its T_{max} cooling rate, its T_{ave} value changed by only -0.01^{o}C decade^{-1}, while its DTR thus decreased by -0.58^{o}C decade^{-1}.

4. Discussion

This section first compares the current results with those in the literature (as described in Section 1) and then offers a hypothesis and supporting data to explain them. Previous studies (e.g., Duffy et al. 2006; LaDochy et al. 2007) have also used 1950-2005 summer (JJA) COOP data and have found some or all of the following all-California current-results: (a) increased T_{ave}-values, (b) asymmetric warming, as T_{min}-values increase faster than T_{max}-values, and (c) thus decreased DTR values.

Current results also show COOP sites in the coastal and/or inland valleys influenced by marine air penetration with JJA increased T_{min}- and decreased T_{max}-values. Previous studies that

have likewise found these results include Nemani et al. (2001) for the SFBA, Christy et al. (2006) and Bonfils and Lobell (2007) for the CenV, and LaDochy et al. (2007) for the SoCAB. While these studies also generally also found decreased JJA DTR values for these valleys, LaDochy et al. (2007) found increased values at 30 of 219 sites. While the current study likewise showed decreased JJA DTR values for all California sites taken together, it found that this arose from combined small DTR-increases at its "inland" sites and large DTR-decreases at its "coastal" sites.

Observational studies have suggested that the summer cooling of JJA T_{max}-values in California were due to increased irrigation (e.g., Christy et al. 2006; Bonfils and Lobell 2007), coastal upwelling (e.g., Bakun 1990; Goodridge 1991), or cloud cover (e.g., Nemani et al. 2001). Modelling studies have also attributed this cooling to either increased upwelling (e.g., Snyder et al. 2003) or irrigation (e.g., Kueppers et al. 2007).

The current hypothesis is that observed coastal-California JJA cooling of T_{max}-values arises from GHG-induced global-warming of "inland" areas, which results in increased sea breeze flow activity, which overwhelms (as discussed below) that warming in "coastal" areas. Note that the hypothesis is consistent with increased upwelling, which increases sea breeze flows and thus coastal stratus.

As sea breeze flows are driven by gradients of ocean-to-inland sea-level pressure p_s, the spatial-distribution of p_s-trend from 1970 to 2006 was calculated from average JJA NCEP reanalysis values at 1700 LT (Fig. 7). Results show pressure increases (up to 0.1 hPa decade^{-1}) in the oceanic Pacific High and decreases (up to -0.3 hPa decade^{-1}) in the central-California Thermal Low. These changes could arise from increased upward motion in the Low due to the GHG-induced warming and the thus induced increased downward motion in the High. The corresponding trend in the gradient of p_s was calculated from the difference between the average-val-

ues in a 5 by 5 deg ocean area off central California (western red square in Fig. 7) and in the similar land area to its east. Results (Fig. 8) showed a trend of 0.02 hPa 100-km^{-1} decade^{-1}, supportive of the hypothesis of an increased sea breeze activity.

Increased sea breeze activity implies increased moisture values in marine-intrusion areas, and thus 1970-2005 trends in 1700 LT T_D values at the NWS sites at SFO (well within the sea breeze intrusion zone) and SEC (near its average eastern boundary) were calculated. Results (Fig. 9) thus show a larger T_D-trend at SFO than at SEC (0.42 vs.0.32^{o}C decade^{-1}, respectively). Christy et al. (2006) found a similar trend at Fresno (also in the CenV, but 100 km southeast of SEC), which was attributed to enhanced agricultural irrigation. The current results indicate that all of the change at coastal SFO, and at least part of it at inland SEC, are due to increased sea breeze activity; the current study did not extend southward to Fresno.

Nemani et al. (2001) showed that increased annual T_D-values over coastal California were related to increased SST-values, and thus the 1950-1975 and 1976-2005 average JJA trends in average SST were calculated for the ocean area of Fig. 1. Results (Fig. 10) showed SST-trends of 0.02 and 0.15^{o}C decade^{-1}, respectively. Increased SSTs could thus also be a factor in the currently-observed increased T_D-values. The 1976-2005 T_D-trend has the same magnitude as the corresponding current all-California T_{ave}-trend, and 1970-2005 T_D-values are correlated with coastal T_{max}-values ($r > 0.8$, not shown).

The sharp increased rate of California SST warming since 1976 (Ebbesmeyer et al. 1990) is believed associated with a concurrent PDO intensification, which has produced more frequent El Niño events (Trenberth and Hoar 1997; McGowan et al. 1998). While Alfaro et al. (2004) and the current study (not shown) showed summer California T_{ave}-values strongly correlated with the PDO, LaDochy et al. (2007) and the current study showed T_{max} uncorrelated with PDO.

While Goodridge (1991), Bereket et al. (2005), Duffy et al. (2006), and LaDochy et al. (2007) have attributed trends in T_{min} and/or T_{ave} to an UHI effect, it could also affect the currently observed T_{max}-increases in areas of the SFBA and SoCAB. Sacramento, Modesto, Stockton, and San José all have experienced growth (DoT 1970) in aerial extent (21 to 59%) and population (40 to 118%), and thus part of their currently observed small increases in JJA T_{max}-values could be partially due to increased daytime UHI-intensity. Without UHI effects, the currently observed JJA SFBA coastal-cooling area might have been expanded to include these sites, as the first three are adjacent to rural airport sites, which showed cooling T_{max}-values due to increased marine influences. In addition, all urbanized sites that showed cooling T_{max}-values probably would show larger trends if UHI effects could be removed.

To determine if GCM models can discern the coastal-cooling effects in the current results, 1950-99 JJA median (of 11 models) GCM 2-m T_{ave}-values over California were determined. Results (Fig. 1) show warming that decreases from $0.13^{o}C$ $decade^{-1}$ at inland California to $0.08^{o}C$ $decade^{-1}$ at coastal areas north of the SoCAB. While this ensemble result thus correctly shows coastal influences on T_{ave}, its coarse spatial resolution may not allow it to sufficiently resolve local topographic features, and thus fine-scale near-surface flow features, necessary to produce the coastal cooling of T_{max}-values seen in current analysis of COOP data.

5. Conclusion

The study evaluated 1948-2004 summer (JJA) mean monthly 2-m air temperatures from 273 COOP sites, with a focus on two California air basins: SoCAB and Central California (i.e., SFBA and northern CenV). The study also focused on the more rapid post-1970 warming period, and its daily T_{min} and T_{max} values were used to produce average monthly values. Trends of these variables were calculated for each site, all sites combined, and coastal and inland subregions. The goal of this study was to elucidate a richer detail of the observed temperature

record than done before, for the potential evaluation of California climate-change models. Spatial distributions of observed temperature trend-values for each air basins were thus constructed, with summertime climatological wind patterns overlaid to aid their interpretation.

Additional analyses included concurrent trends of T_D values at the NWS sites at SFO and SEC airports at 1700 LT. Mean-monthly JJA SSTs at a 2.5-degree grid resolution were also used to construct 1950-2005 average trends. The 1970 to 2006 spatial-distribution of trends of the coastal-to-inland gradient of sea-level pressure-p_s to estimate changes in sea breeze activity were calculated by use of average JJA NCEP reanalysis values at 1700 LT. GCM outputs of 2-m JJA T_{ave}-values from 11 models for 1950-99 on a 2 by 2 deg grid over California were also obtained from the IPCC archive, and average values interpolated to a 0.5 by 0.5 degree grid.

Results for all California COOP sites together showed increased JJA T_{ave}-values; asymmetric warming, as T_{min}-values increase faster than T_{max}-values; and thus decreased DTR values. The spatial distribution of observed SoCAB and SFBA 1970-2004 JJA T_{max} values exhibited a complex pattern, with cooling in low-elevation coastal-areas open to marine air penetration and warming at both inland and higher-elevation coastal areas. While previous studies also found decreased JJA DTR values for these valleys, the current study showed that the decrease arose from small increases at “inland” sites combined with large decreases at “coastal” sites.

Previous studies have suggested that the cooling of JJA T_{max}-values in coastal California were due to increased irrigation, coastal upwelling, or cloud cover, while the current hypothesis is that it arises from GHG-induced global-warming of “inland” areas, which results in increased sea breeze flow activity, which overwhelms that warming in “coastal” areas. This is consistent with increased upwelling, which increases sea breeze flows and thus coastal stratus. The spatial-distribution of p_s-trend from 1970 to 2006 at 1700 LT showed pressure increases in the oceanic Pacific High and decreases in the central-California Thermal Low. The corresponding trend in

the gradient of p_s showed a trend of 0.02 hPa 100-km^{-1} decade^{-1}, supportive of the hypothesis of increased sea breeze activity.

Calculated 1970-2005 trends in 1700 LT T_D values at showed a larger value at coastal SFO than at inland SEC. A similar trend, previously found at Fresno, was attributed to enhanced agricultural irrigation, and thus the current results indicate that all the SFO changes, and some of it at SEC, are due to increased sea breeze activity. Calculated 1976-2005 average JJA trends in SST showed a value of 0.15^{o}C decade^{-1}, which could also be a factor in the currently-observed increased T_D-values.

Previous studies have also attributed trends in California JJA T_{min} and/or T_{ave} to UHI effects, which could also affect the currently observed T_{max}-increases. As CenV cities have experienced growth in aerial extent and population, part of their currently observed small increases in T_{max} could be due to increased daytime UHIs. Without this effect, the currently observed SFBA coastal-cooling area might have been expanded to include these sites. All urbanized sites with cooling T_{max}-values probably would show even larger trends, if UHI effects could be removed.

GCM model 1950-99 JJA median T_{ave}-values showed warming that decreases from 0.13^{o}C decade^{-1} at inland California to 0.08^{o}C decade^{-1} at coastal areas. While this correctly shows coastal influences on T_{ave}, its coarse spatial resolution does not allow it to sufficiently resolve the local topographic, and thus fine-scale near-surface flow, features necessary to produce the coastal cooling of T_{max}-values in current analysis. California coastal cooling of annual T_{ave}-values, however, is seen as a single data point in the global 2001 IPCC observational data set (Jin 2004).

Additional observational sites and/or downscaled model results (to mesoscale models with 1–10 km grids resolution) are thus necessary to determine the fine-scale structure and more precise boundaries between the adjacent warming and cooling areas found in the current results. In addition, additional SST, sea breeze (e.g., onshore wind speed and cloud cover), agricultural-irrigation, and UHI effects need further analysis and model simulations.

The most significant result of the current study is that the expected GHG driven global warming of summer T_{max}-values in the eastern inland CenV and Sierra Nevada foothills may have produced enhanced cool-air sea breeze intrusions, and thus may have induced the currently observed cooling of summer T_{max}-values in low-elevation coastal basins. This regional effect appears to coexist with the GHG-induced increases in California-wide daily T_{max}-, T_{min}-, and T_{ave}-values and with increases in summer T_{min}-values in both basins.

The observed coastal cooling may thus be an example of a regional "reverse-reaction" to the warming. Significant societal impacts in California may result from this observed "reverse-reaction", e.g., decreased water supply, as summer mountain snowmelt will shift into winter rain runoff, with its increased soil absorption during flow to valley reservoirs. Agricultural production will increase or decrease, e.g., wine grape production will increase in the cooling valleys north of San Francisco. Other beneficial effects due to the reduced summer T_{max}-values include decreased maximum O_3 levels, which will occur due to resulting reduced: fossil-fuel usage for cooling, natural hydrocarbon production, and photochemical photolysis rates. Human thermal-stress rates and mortality will also decrease.

While similar GHG-induced "reverse-reactions" could be expected in other subtropical low-elevation coastal regions, similar impacts might also exist in areas of high topography, as with the cooling found along the California-Nevada border by Christy et al. (2006) and LaDochy

et al. (2007). Such possibilities require further investigation by additional regional-scale data analyses and/or dynamically-downscaled numerical modeling.

Acknowledgments.

The authors would like to thank the School of Engineering, Santa Clara University for funding the lead author. We also acknowledge the Program for Climate Model Diagnosis and Intercomparison (PCMDI) for collecting and archiving CMIP3 model output and the WCRP Working Group on Coupled Modelling (WGCM) for organizing the model-data analysis. The WCRP CMIP3 multi-model dataset is supported by the Office of Science, U.S. Department of Energy, under Contract No. DE-AC02-05CH11231.

References

Abatzoglou, J. T., 2008: personal communication.

Abatzoglou, J. T., K. T. Redmond, and L .E. Edwards, 2008: Classification of regional climate variability in the state of California. *J. Appl. Met. and Climatology*, in preparation.

Alfaro, E.J., A. Gershunov, and D. Cayan, 2006: Prediction of summer maximum and minimum temperature over the central and western United States: The role of soil moisture and sea surface temperature. *J. Climate*, **19(8)**, 1407-1421, doi: 10.1175/JCLI3665.1.

Bakun, A., 1990: Global climate change and intensification of coastal ocean upwelling. *Science*, **247,** 198–201.

Bereket, L., D. Fabris, J. E. Gonzalez, S. Chiappari, N. L. Miller, and R. Bornstein, 2005: Climatology temperature mapping for California urban heat islands. *Bulletin Amer. Meteor. Soc.*, **86**, 1542-1543.

Betts, R. A., 2001: Biogeophysical impacts of land use on present-day climate: near-surface temperature change and radiative forcing. *J. Atmos. Sci*. *Lett*, **2,** 39–51.

Blumenthal, D. L., T. B. Smith, D. E. Lehrman, R. A. Rasmussen, G. Z. Whitten, and R. A. Bazter, 1985: Southern San Joaquin Valley ozone study. Sonoma Technology Inc. Final Rep., 143 pp.

Bonfils, C., and D. Lobell, 2007: Empirical evidence for a recent slowdown in irrigation-induced cooling. *Proc. Natl. Acad. Sci.*, doi:10..1073/pnas.0700144104.

Bonfils, C., and P. B. Duffy, 2007: Comments on "Methodology and results of calculating central California surface temperature trends: Evidence of human-induced climate change?" by J. R. Christy et al., *J. Clim*., **20,** 4486-4489.

Bornstein, R. D., 1968: Observations of the urban heat island effect in New York City. *J. Appl. Meteor.*, **7,** 575–582.

Boucouvala, D., R. Bornstein, J. Wilkinson, and D. Miller, 2003: MM5 simulations a SCOS97-NARSTO episode. *Atmos. Environ.,* **37,** S95–S117.

CARB, 1989: Proposed identification of districts Affected by transported air pollutants. California Air Resources Board, Research Report, 92 pp.

Chase, T. N, R. A. Pielke, Sr., T. G. F Kittel, R. R. Nemani, and S. W. Running, 2000: Simulated impacts of historical land cover changes on global climate in northern winter. *Clim. Dyn.*, **16,** 93–105.

Christy, J. R., W. B. Norris, K. Redmond, and K. P. Gallo, 2006: Methodology and results of calculating Central California surface temperature trends: Evidence of human-induced climate chage? *J. Climate,* **19,** 548–563.

Duffy, P. B., C. Bonfils, and D. Lobell (2007), Interpreting Recent Temperature Trends in California, *Eos Trans. AGU*, **88,** 409-410.

Defries, R. S., L. Bounoua, and G. J. Collatz, 2002: Human modification of the landscape and surface climate in the next fifty years. *Global Change Biol.*, **8**, 438–58.

DoT, 2000: US Department of Transportation, Highway administration. [available online at http://www.fhwa. dot.gov/ohim/hs00/hm72.]

Ebbesmeyer, C. C., D. R. Cayan, D. R. McLain, F H. Nichols, D. H. Peterson, K. T. Redmond, 1990: 1976 step in the Pacific climate: forty environmental changes between 1968–1975 and 1977–1984. In: Betancourt JL, Tharp VL (eds) Proc 7th Annu Pac Clim (PACLIM)

Workshop. Interagency Ecol Stud Prog Tech Rep 26, California Department of Water Resources, Sacramento, CA, p 115–126.

Gallo, K. P., A. L. McNAB, T. R. Karl, J. F. Brown, J. J. Hood, and J. D. Tarpley, 1993: The use of a vegetation index for assessment of the urban heat island effect. *Int. J. Remote Sens.*, **11,** 2223–2230.

Gilliland, R. P., 1980: The structure and development of the California heat trough. M.S. thesis, Dept. of Meteorology, San Jose State University, 90 pp.

Giorgis, R. B., 1983: Meteorological influence on oxidant distribution and transport in the Sacramento Valley. Ph.D thesis, University of California at Davis, 124 pp.

Goodridge, J. D., 1991: Urban bias influence on long-term California air temperature trends. *Atmos. Environ.,* **26B,** 1–7.

Hayes, T. P., J. J. R. Kinney, and N. J. M. Wheeler, 1984: California surface wind climatology. CARB Res. Rep., 79 pp.

Herbert, T. D., and J. D. Schuffert, 2001: Collapse of the California Current During Glacial Maxima Linked to Climate Change on Land, *Science*, **293,** 71-76.

Hickey, B. M., 1979: The California Current system - hypotheses and facts. *Prog. Oceanogr.*, **8,** 191-279.

Jin, M., 2004: Analyzing skin temperature variations from long-term AVHRR. *Bull. Am. Meteor. Soc.*, **85,** 587-600.

Karl, T. R., P. D. Jones, R. W. Knight, G. Kukla, N. Plummer, V. Razuvayev, K. P. Gallo, J. Lindseay, R. J. Charlson, and T. C. Peterson, 1993: A new perspective on recent global

warming: Asymmetric trends of daily maximum temperature. *Bull. Am. Meteor. Soc.*, **74,** 1007–1023.

Kueppers, L. M., M. A. Snyder, and L. C. Sloan, 2007: Irrigation cooling effect: Regional climate forcing by land-use change. *Geophys. Res. Lett.*, **34,** L03703.

LaDochy, S., R. Medina, and W. Patzert, 2007: Recent California climate variability: spatial and temporal patterns in temperature trends *Climate Research,* **CR 33,** 159–169.

Landsberg, H. E., 1970: Man-made climate changes. *Science,* **170,** 1265–1274.

Lawton, R. O., U. S. Nair, R. A. Pielke, Sr., and R. M. Welch, 2001: Climatic Impact of tropical lowland deforestation on nearby montane cloud forests. *Science,* **294,** 584-587.

Lobell, D. B., G. Bala, C. Bonfils, and P. B. Duffy 2006: Potential bias of model projected greenhouse warming in irrigated regions, *Geophys. Res. Lett.*, **33,** L13709, doi:10.1029/2006GL026770.

MacKay, K., 1997: Ozone Over San Francisco: Means and patterns during pollution episodes. San Jose State Univ., Research Report, Dept. of Meteorology, 55 pp.

Maurer, E. P., 2007: Uncertainty in hydrologic impacts of climate change in the Sierra Nevada, California under two emissions scenarios, *Climatic Change,* **82,** 309-325**,** doi: 10.1007/s10584-006-9180-9.

McElroy, J. L., and T. B. Smith, 1991: Lidar descriptions of mixing-layer thickness characteristics in a complex terrain/coastal environment *J. Appl. Meteor.*, **30,** 585–597.

McGowan, J. A., D. R. Cayan, and L. M. Dorman, 1998: Climate-ocean variability and ecosystem response in the northeast Pacific. *Science,* **281,** 210–217.

McGregor, H. V., M. Dima, H. W. Fischer, and S. Mulitzal, 2007: Rapid 20th-Century Increase in Coastal Upwelling off Northwest Africa. *Science*, **315,** 637–639.

Miller, N. L., and N. J. Schlegel, 2006: Climate change projected fire weather sensitivity: California Santa Ana wind occurrence. *Geophys. Res. Lett.,* **33,** L15711.

Mintz, Y., 1984: The sensitivity of numerically simulated climates to land-surface boundary conditions. In *The Global Climate*, Houghton, J., Cambridge Univ. Press, 79–105.

Nair, U. S., R. O. Lawton, R. M. Welch, and R. A. Pielke, Sr., 2003: Impact of land use on Costa Rican tropical montane cloud forests: Sensitivity of cumulus cloud field characteristics to lowland deforestation. *J. Geophys. Res.*, **108,** 4206, doi:10.1029/ 2001JD001135.

Nemani, R. R., M. A. White, D. R. Cayan, G. V. Jones, S. W. Running, and J. C. Coughlan, 2001: Asymmetric warming over coastal California and its impact on the premium wine industry. *Climate Research*, **19,** 25–34.

Pielke Sr., R. A., C. Davey, D. Niyogi, S. Fall, J. Steinweg-Woods, K. Hubbard, X. Lin, M. Cai, Y.-K. Lim, H. Li, J. Nielsen-Gammon, K. Gallo, R. Hale, R. Mahmood, S. Foster, R. T. McNider, and P. Blanken, 2007: Unresolved issues with the assessment of multi-decadal global land surface temperature trends. *J. Geophys. Res.*, **112,** D24S08, doi:10.1029/2006JD008229.

Pielke, Sr., R. A., G. Marland, R. A. Betts, T. N. Chase, J. L. Eastman, J. O Niles, D. Niyogi, and S. Running, 2002: The influence of land-use change and landscape dynamics on the climate system: relevance to climate-change policy beyond the radiative effect of greenhouse gases. *Philosophical Trans. of Royal Soc. of London-A,* **360,** 1705–1717.

Pielke, Sr., R .A., C. Davey, D. Niyogi, S. Fall, J. Steinweg-Woods, K. Hubbard, X. Lin, M. Cai, Y.-K. Lim, H. Li, J. Nielsen-Gammon, K. Gallo, R. Hale, R. Mahmood, S. Foster, R. T. McNider, and P. Blanken, 2007: Unresolved issues with the assessment of multi-decadal global land surface temperature trends. *J. Geophys. Res*., **112**, D24S08, doi:10.1029/2006JD008229.

Pon, B., D. M. Stamper-Kurn, C. K. Smith, and H. Akbari, 2000: Existing climate data sources and their use in heat island research. LBNL Tech. Rep. LBL41973, 20 pp.

Root, H. E., 1960: San Francisco, the air conditioned city. *Weatherwise,* **13,** 47–54.

Seaman, N. L., D. R. Stauffer, and A. M. Lario-Gibbs, 1995: A multiscale four-dimensional data assimilation system applied in the San Joaquin Valley during SARMAP. Part I: modeling design and basic performance characteristics. *J. Appl. Meteor.*, **34,** 1739–1761.

Simpson, J. J., 1983: Large-scale thermal anomalies in the California Current during the 1982-1983 El Ninio, *Geophys. Res. Lett.,* **10,** 917-940.

Smith, T. M., and R. W. Reynolds, 2003: Extended reconstruction of global sea surface temperature based on COADS data. *J. Climate*, **16,** 1495–1510.

Stenchikov, G. L., and A. Robock, 1995: Diurnal asymmetry of climatic response to increased CO_2 and aerosols: Forcings and feedbacks. *J. Geophys. Res.,* **100,** 26211–26227.

Snyder, M. A., L. C. Sloan, N. S. Differbaugh, and J. L. Bell, 2003:Future climate change and upwelling in the California Current. *Geophys. Res. Lett.*, **30,** 1823, doi:10.1029/2003GL017647.

Switzer, P., 2008: Personal communication.

Trenberth, K. E.,and T. J. Hoar, 1997: El Nino and climate change.*Geophys Res Lett ,* **24,** 3057–3060

Walters, J. T., R. T. McNider, X. Shi, W. B Norris, and J. R. Christy 2007: Positive surface temperature feedback in the stable nocturnal boundary layer, *Geophys. Res. Lett.*, **34,** L12709, doi:10.1029/2007GL029505

Williams, W., and R. DeMandel, 1966: Land-sea Boundary Effects on Small Scale Circulations. SJSU Res. Rep., Meteor. Dept., 97 pp.

Zhang, H., 1997: Henderson-Sellers, A. & McGuffie, K. Impacts of tropical deforestation. Part II: The role of large scale dynamics. *J. Climate,* **10,** 2498–2522.

List of Figures

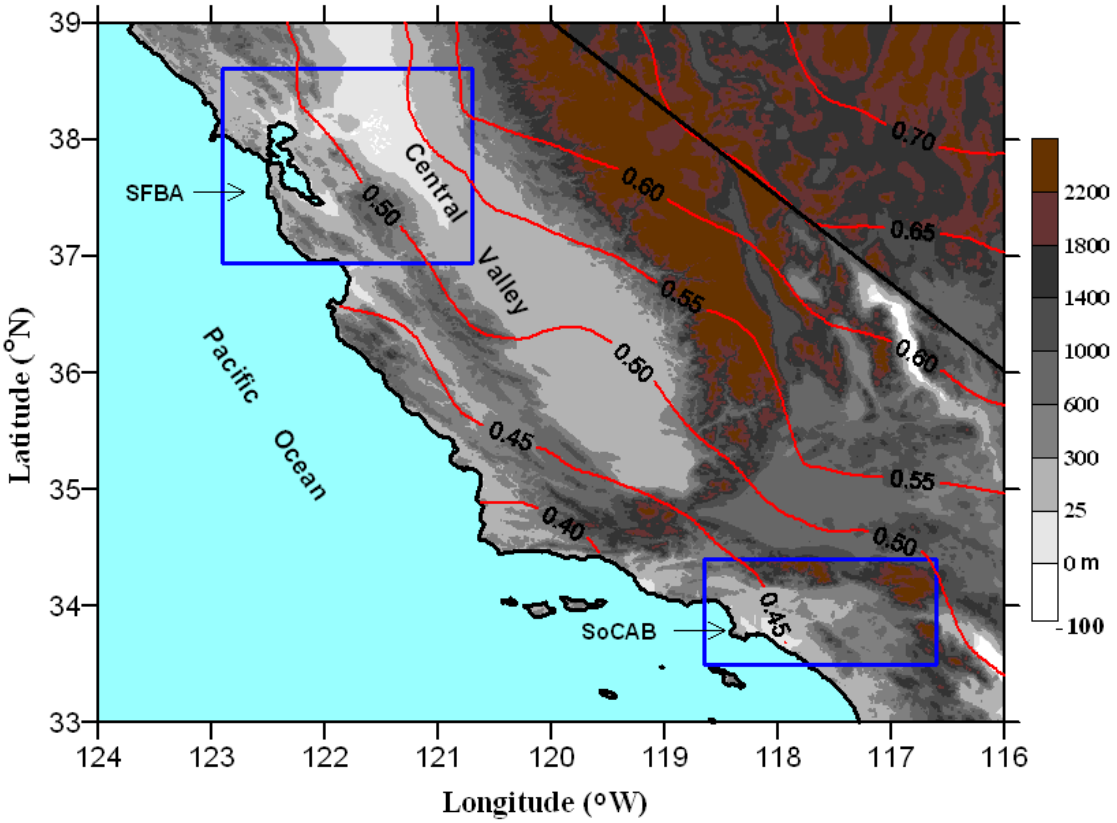

FIG. 1. California topography (m), study areas of Figs. 2 and 3 (blue boxes), and summer daily-average 2-m 1950-1999 temperature-change (^{o}C)..

(a)

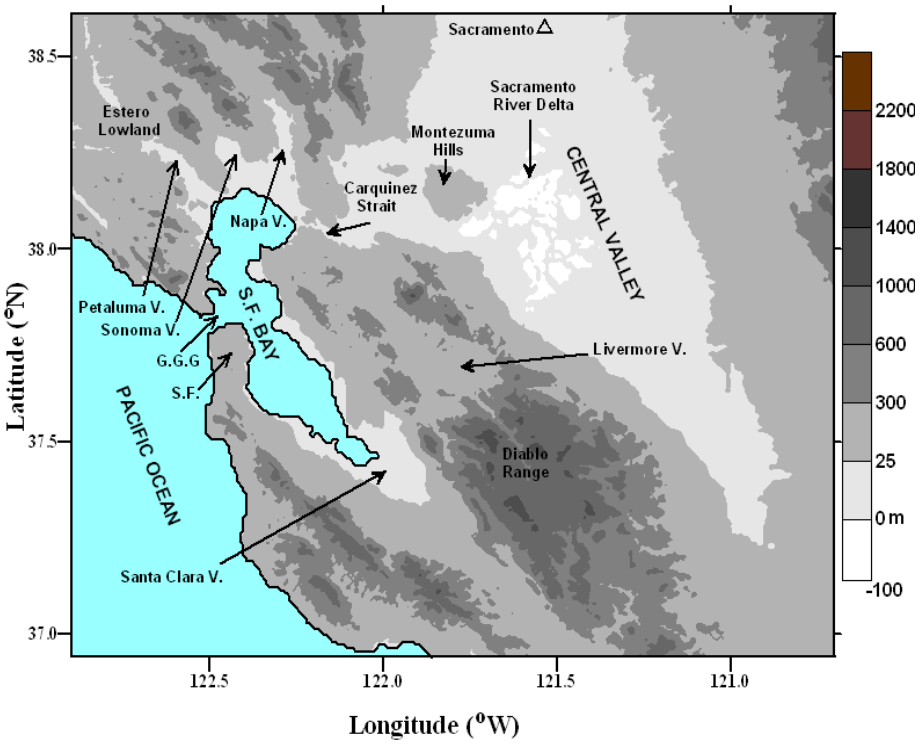

(b)

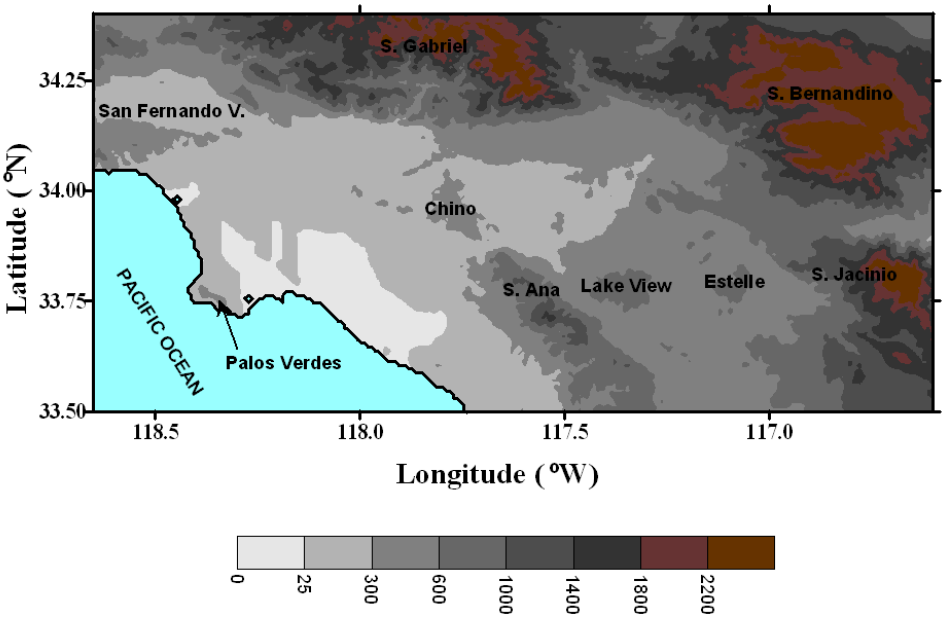

FIG. 2. Topographic heights (m) for: (a) SFBA and (b) SoCAB.

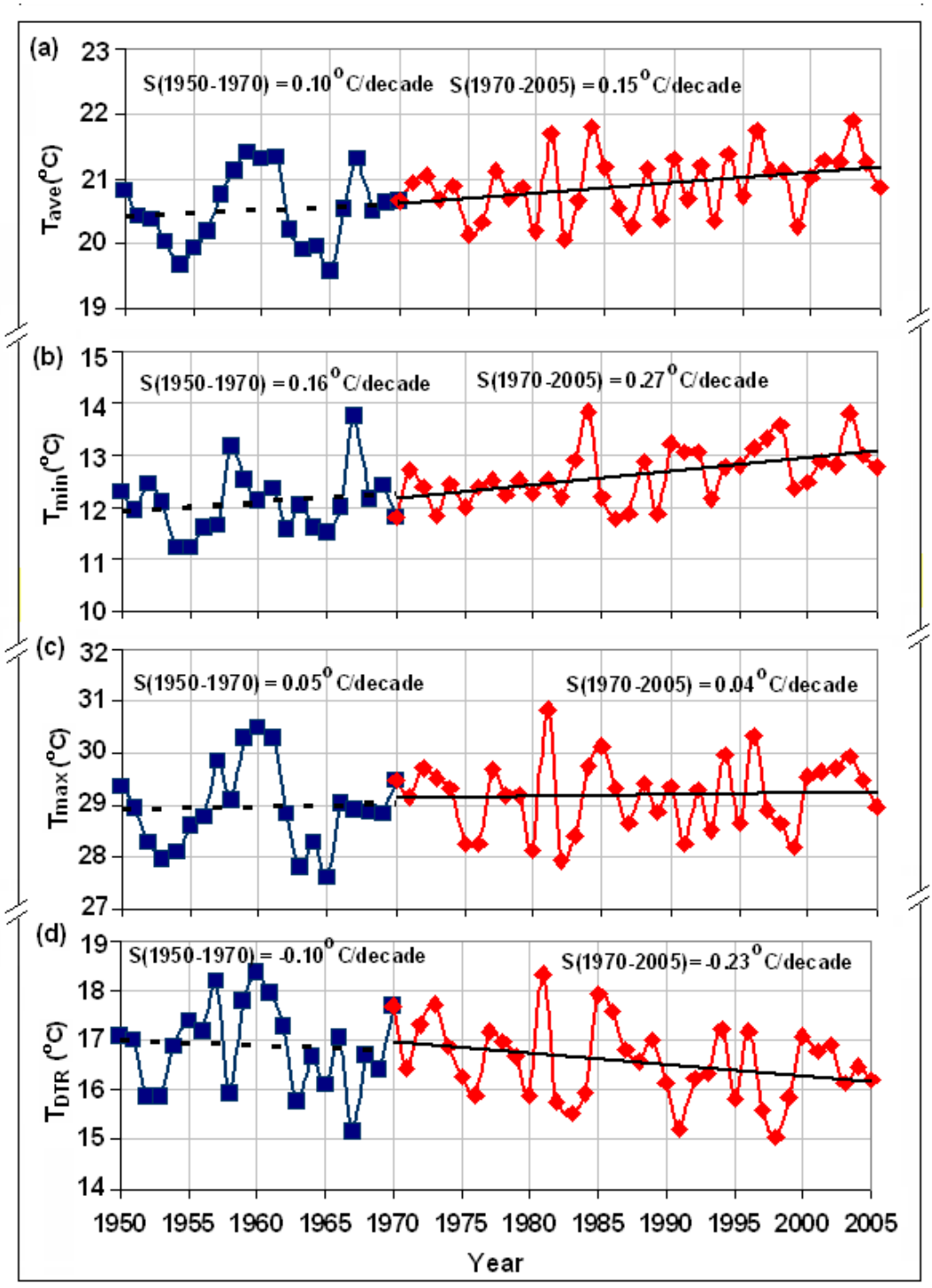

FIG. 3. Summertime California trends (^{o}C decade^{-1}) of 2-m temperatures for 1948-1970 and 1970-2005: (a) maximum, (b) minimum, and (c) daily temperature range (DTR).

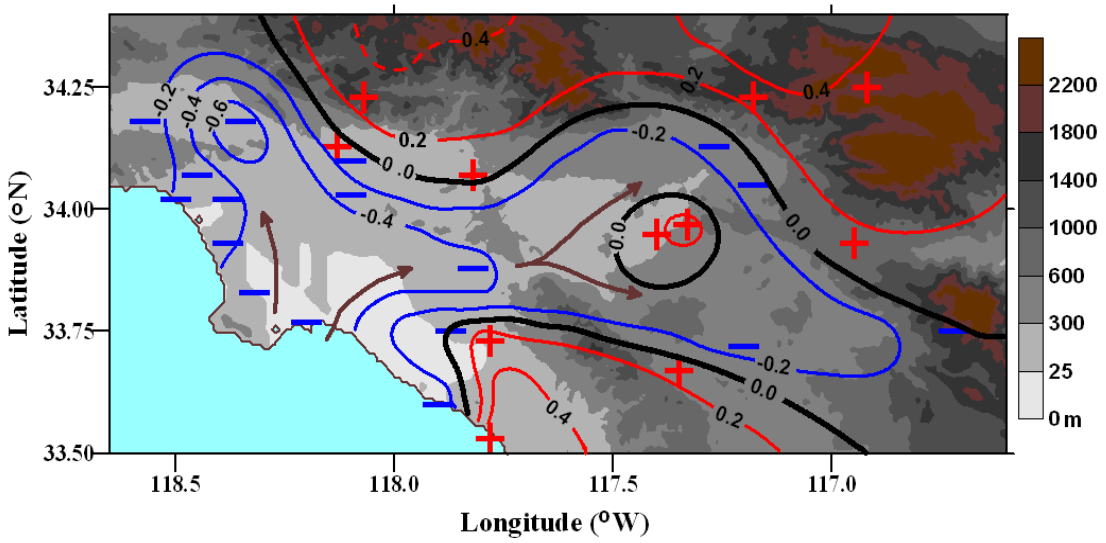

FIG. 4. Spatial distribution of trends in SoCAB 2-m summertime maximum-temperatures (^{o}C decade^{-1}) for 1970-2005; arrows indicate predominant summertime flow-patterns, pluses/minuses (+/-) warming/cooling stations, and isopleths are as follows: blue/red for cooling/warming areas, red dashed for extrapolated warming areas, and black for zero-change.

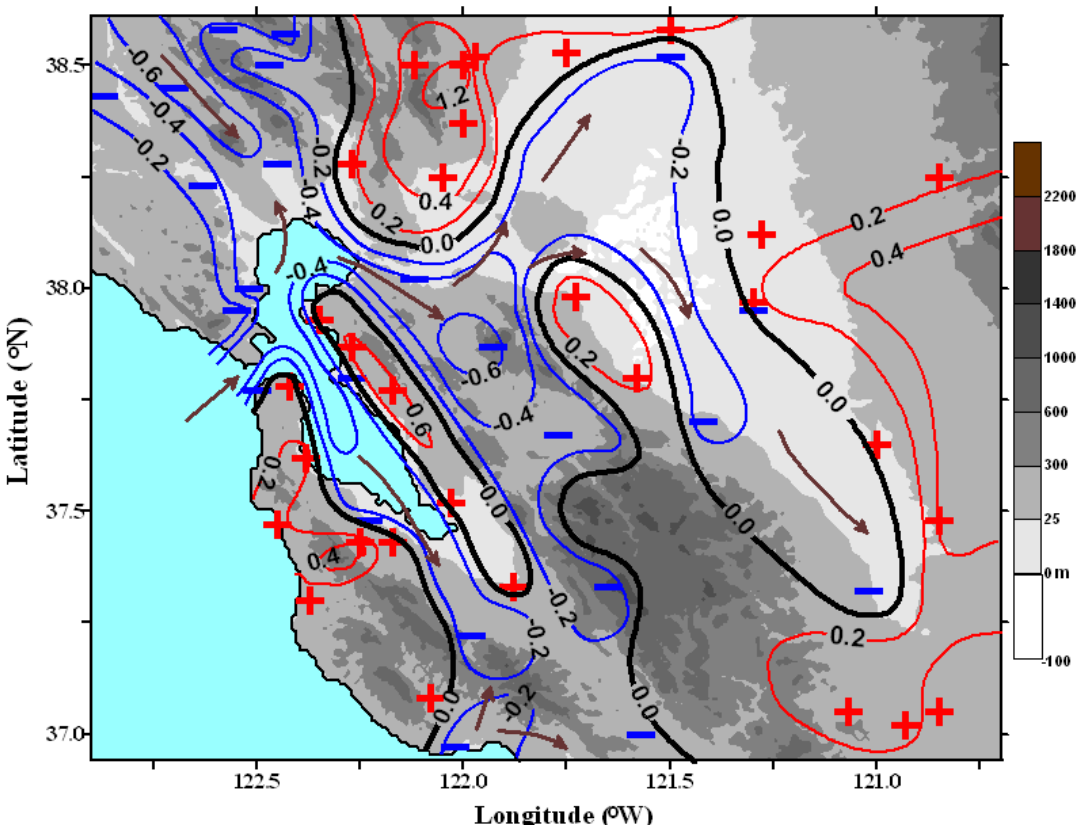

FIG. 5. Same as Fig. 4, but for SFBA.

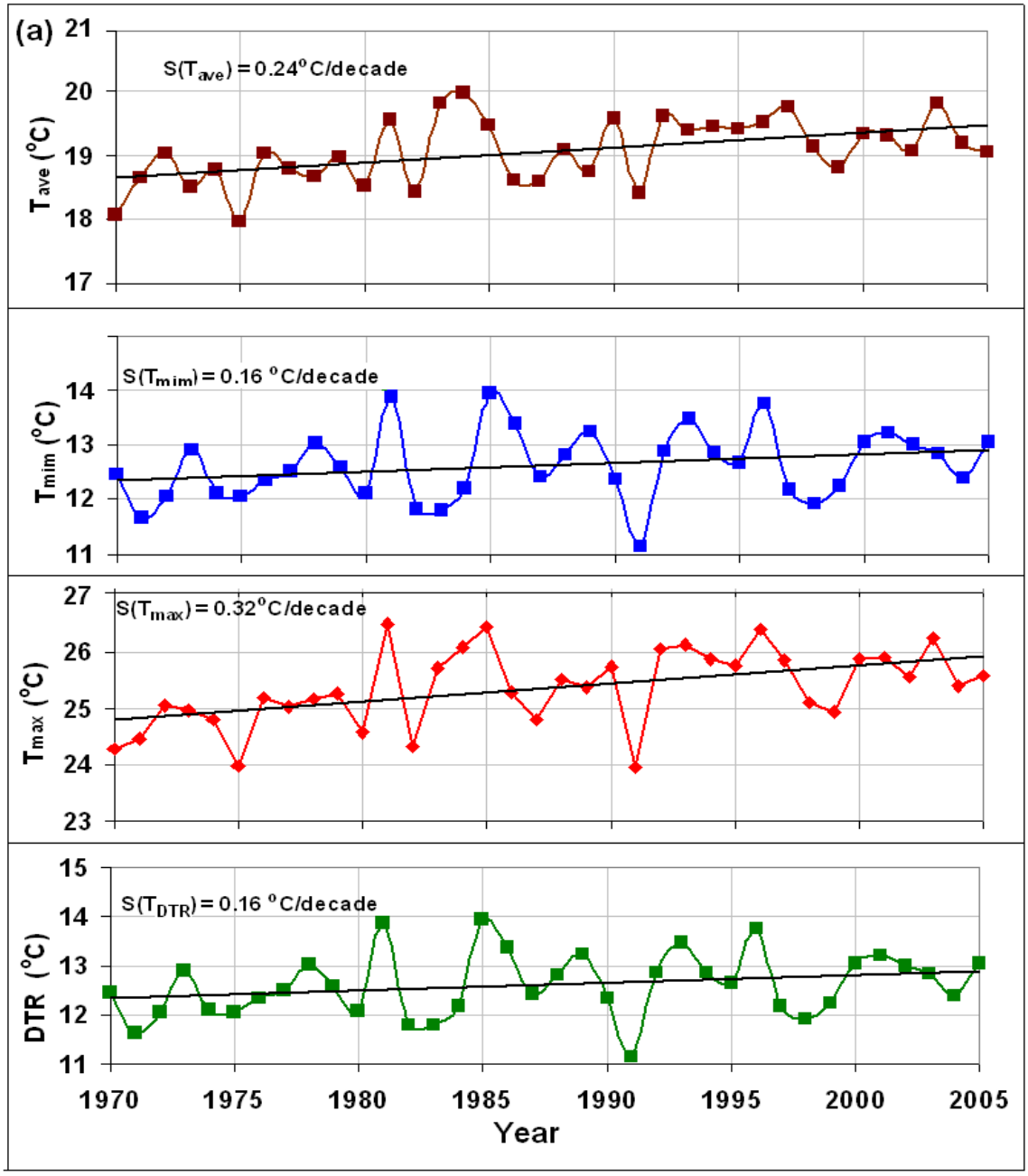

FIG. 6a. Combined SFBA and SoCAB 1950-1970 and 1970-2005 summertime trends (^{o}C decade^{-1}) of maximum and minimum temperatures and of daily temperature range (DTR) for warming areas.

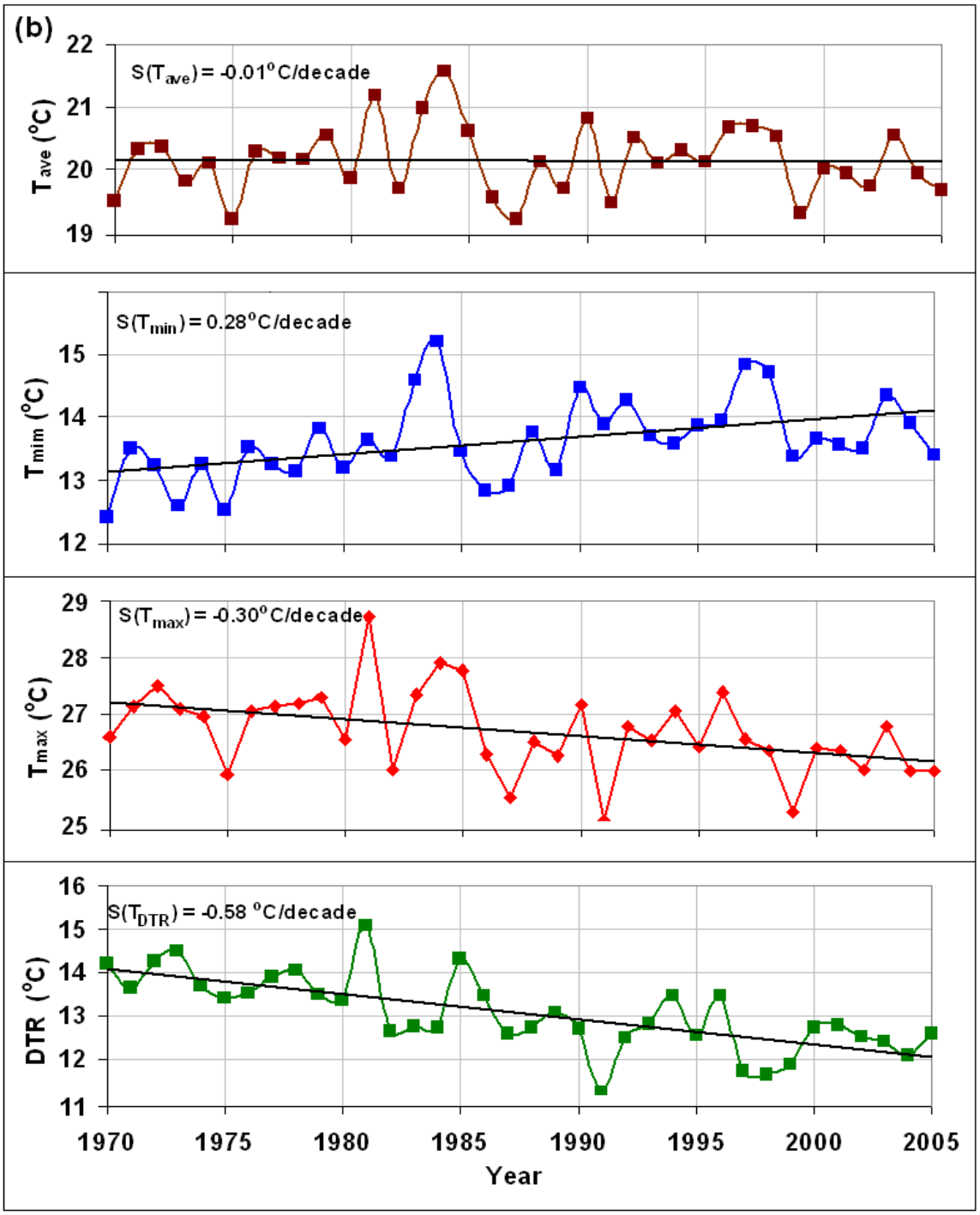

FIG. 6b. Combined SFBA and SoCAB 1950-1970 and 1970-2005 summertime trends (^{o}C decade^{-1}) of maximum and minimum temperatures and of daily temperature range (DTR) for cooling areas.

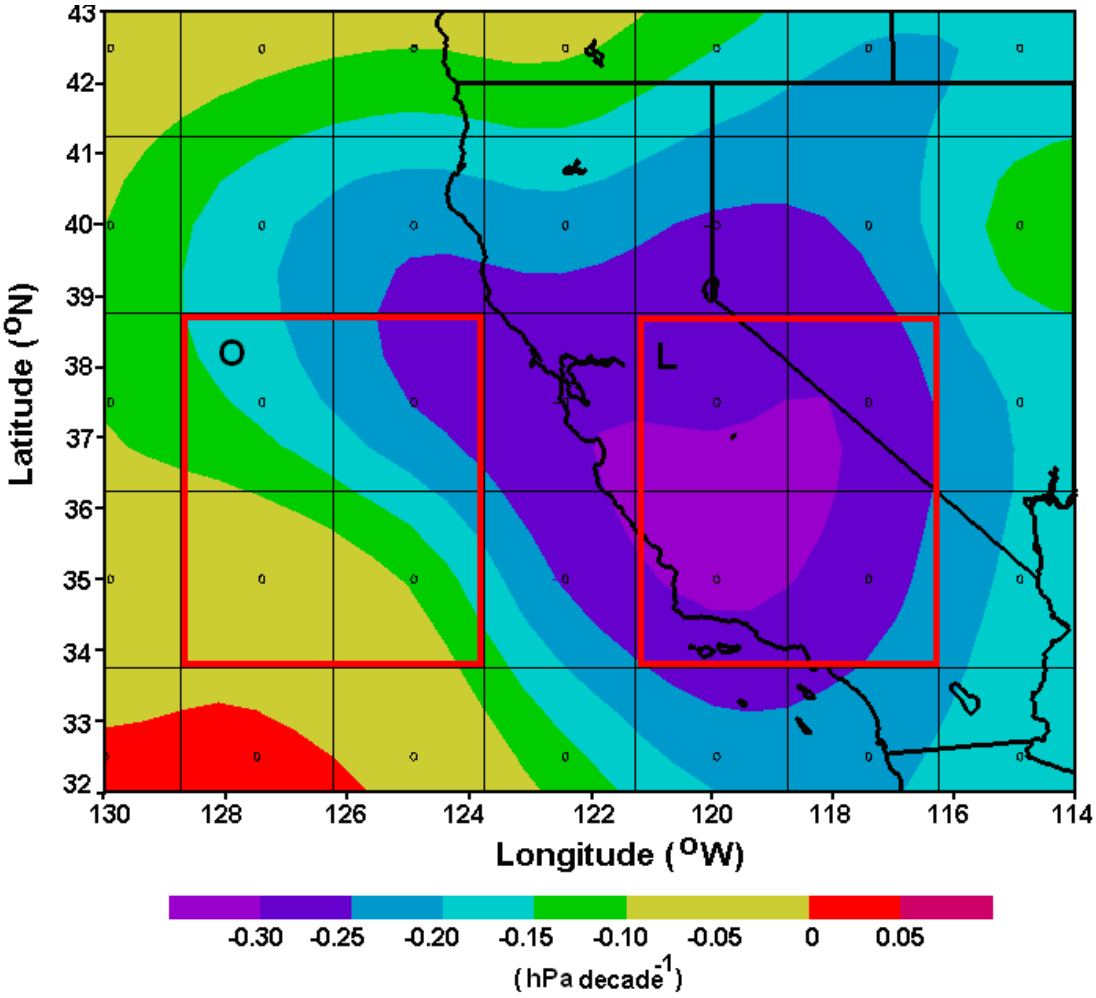

FIG. 7. Trend in 2.5 degree NCEP-reanalysis summertime sea level pressures (hPa/decade) at 0000 UTC for 1970-2005; boxes represent averaging-areas for Fig. 9.

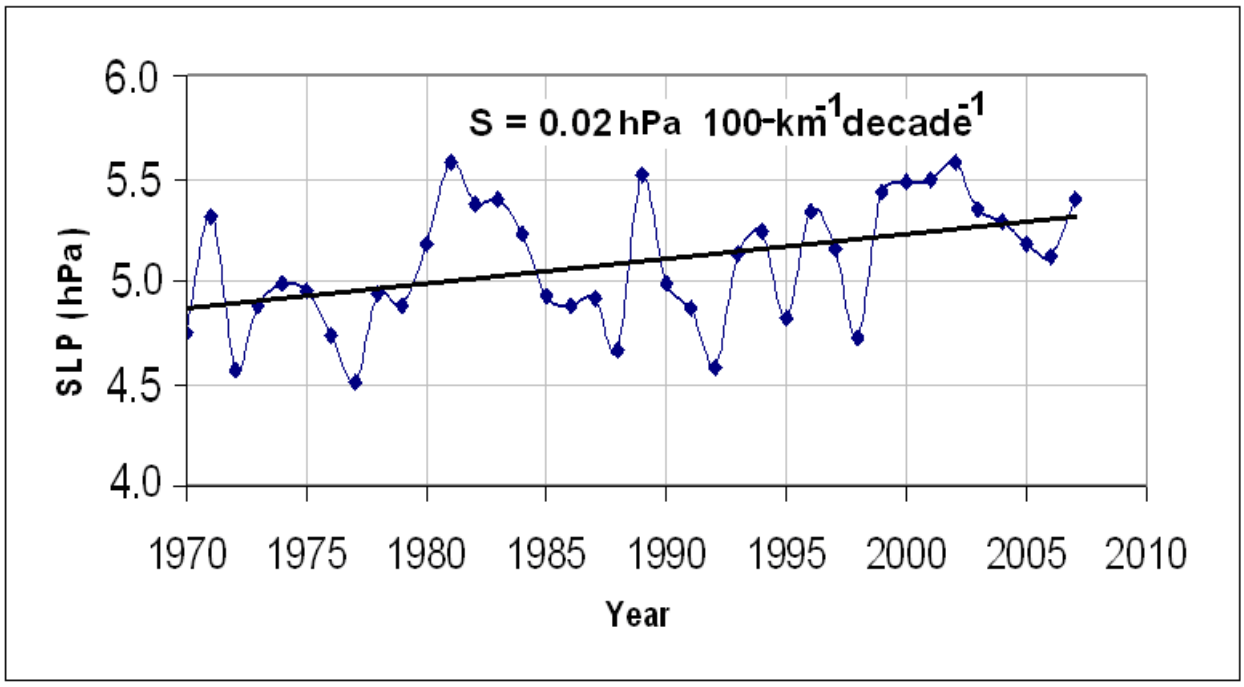

FIG. 8. Trend in ocean minus land sea level pressure gradient (hPa 100-km^{-1} decade^{-1}) between areas in boxes of Fig. 7.

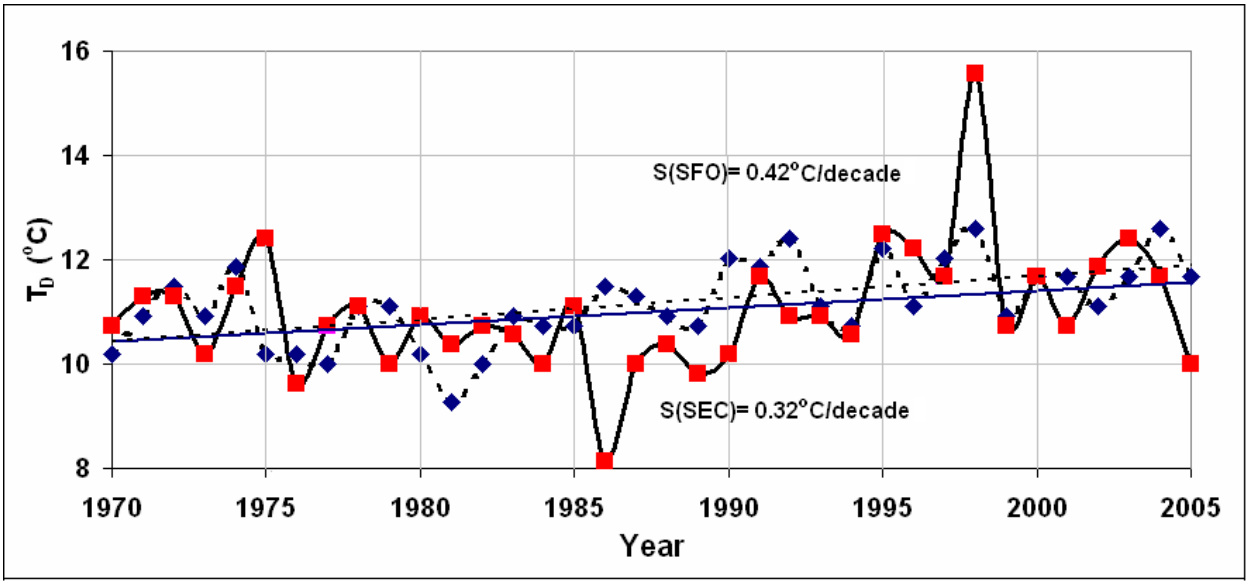

FIG. 9. Summertime 1700 LT T_D-trends (^oC $decade^{-1}$) for SFO (dashed line) and SEC (solid line) airports.

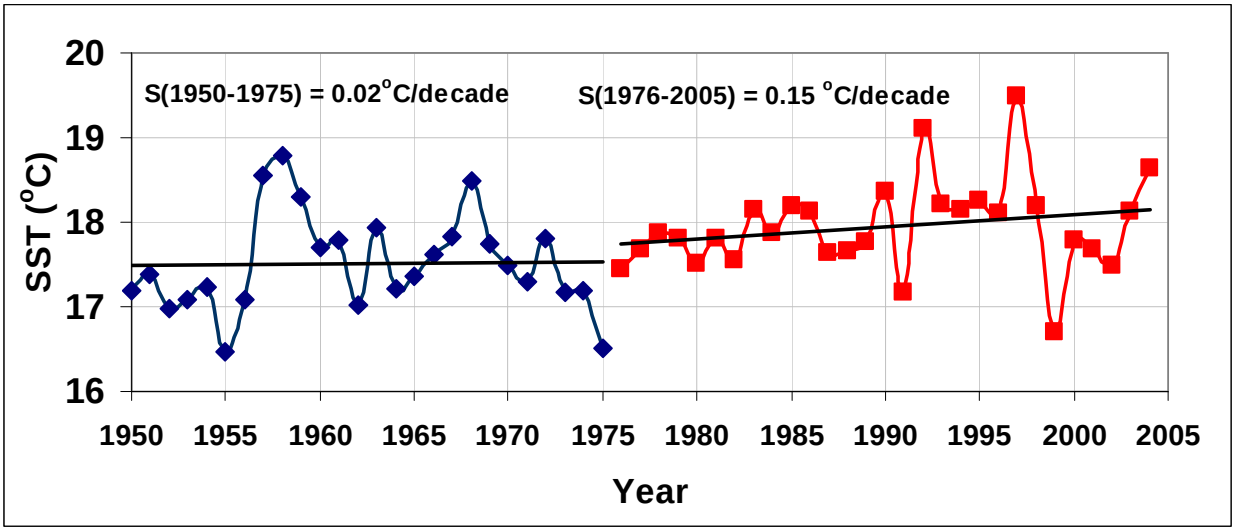

FIG. 10. Trend in summertime average SSTs (^{o}C decade^{-1}) for 1970-2005 in ocean area of Fig. 1.